Investigating the Effect of Histone Demethylase KDM6B Inhibitor GSK-J4 on Cell Surface Levels of Chemokine Receptor CCR7

Malcolm Alencar
malcolm@alencar.se

under the direction of
Dr. Laia Sadeghi
Dept. of Laboratory Medicine
Karolinska Institutet

Research Academy for Young Scientists
July 13, 2022

Abstract

Mantle cell lymphoma is a rare and agressive form of cancer which is usually discovered in either stage III or IV. Although progress is being made in the discovery of new therapies, there are no curative therapies available at the moment, incentivizing further research into new therapies. Mantle cell lymphoma finds protection from chemotherapy as well as an optimum for proliferation in the lymph nodes. In transportation to the lymph nodes, cell surface receptor CCR7 has been identified as a central, and subsequently as a potential therapeutical target. Expression of CCR7 has been linked to overexpression of lysine demethylase KDM6B as it promotes development of euchromatin in the region of CCR7's transcription, which grants transcriptional machinery access. GSK-J4 is characterized as a specific KDM6B inhibitor and the study has thus through qPCR and FACS examined the effect on both translation and transcription of CCR7 in a mantle cell lymphoma cell line which has been treated with GSK-J4. Results did not acheive statistical significance as a result of low sample sizes due to time constraints. Results could indicate a decrease in both translation and transcription of CCR7 as a result of GSK-J4 treatment, but further studies would need to confirm this by achieving statistical significance before any meaningful conclusions can be drawn.

Acknowledgements

First and foremost I would like to express my gratitude to Dr. Laia Sadeghi who guided me through this project. Without her expertise and advice this paper would not have been possible. Further, I would like to thank my lab partner Lif Wilsby for the endless brainstorming and help offered throughout this project. Thanks to Karolinska Institutet for so graciously allowing us to conduct our research in their facilities and a big thanks to all of the amazing students at Rays* for their relentless wit, motivation and energy, something which has greatly influenced not only this project but me personally. A special thanks to the wonderful N16's who stood by my side like family throughout the duration of the project. Thank you to the organizers, Rays – for Excellence, for giving me the opportunity of participating in this years edition of Rays*. Lastly, thank you to the collaborative partners AstraZeneca, Olle Engkvists Stiftelse, Svenska Tekniska Vetenskapsakademin i Finland, Tekniska Museet and Beijerstiftelsen, without them Rays* would not be possible.

Contents

List of Abbreviations

CCR7 C-C Chemokine Receptor 7.

cDNA Complimentary DNA.

DMSO Dimethyl sulfoxide.

Event Detected cell signals in FACS.

EZH2 Enhancer of zeste homolog 2.

H3K27me3 Tri-methylation of lysine 27 on histone H3.

H3K4me3 Tri-methylation of lysine 4 on histone H3.

KDM6B Lysine Demethylase 6B.

LPS Lipopolysaccharide.

MCL Mantle Cell Lymphoma.

NFkB Nuclear Factor Kappa light-chain-enhancer of activated B cells..

qPCR Quantitative Real Time PCR.

1 Introduction

Lymphomas are a form of cancer caused by malignant tumors in the hematopoietic system, consisting of tissue in the lymph nodes, bone marrow and the spleen[1]. Lymphomas are categorized into two major groups, Hodgkin and non-Hodgkin lymphomas. Hodgkin lymphomas are usually limited to the lymph nodes while non-Hodgkin lymphomas generally affect the lymph nodes, spleen and extranodal targets like the stomach[2].

1.1 Mantle Cell Lymphoma

Mantle cell lymphoma (MCL) is a rare and aggressive form of non-Hodgkin B-cell lymphoma caused by a rearrangement in the chromosome. A translocation between chromosome 11 and 14 t(11;14) leads to an over expression of cyclin D1, a protein regulating cell cycle and metabolism[3]. Overexpression of cyclin D1 in B-cells can lead to inactivation of tumor supressor genes, leading to an unregulated proliferation of the malfunctioning B-cells[3]. By diagnosis, MCL has often reached stage III or IV and dissipated past the lymph nodes to bone marrow and splenic tissue[3]. Thus far no curative treatment is available with patient life expectancy of 5 – 7 years [3]. WHile several new therapies are in clinical trials targeting a wide range of cellular mechanisms in MCL cells, these are not demonstrating curative effects nor preventing relapse[4]. Reviews of the field have thus suggested precision therapy as a focus in the search for a curative treatment for MCL [4].

1.2 Cellular Translocation

B-cell migration is necessary for the long term proliferation of lymphomas[2]. Migration is primarily controlled by cytokines and chemokines and the detection of chemokines in B-cells is responsible for the transportation of B-cells throughout the lymphatic system. Specifically, the cell surface receptor C-C chemokine receptor 7 (CCR7) aids the transportation of B-cells to the lymph nodes and enables the detection and subsequent targeting of infecting agents CCR7 has been showed to be up regulated in MCL cells compared

to normally operating B-cells. Furthermore, it has been demonstrated that anti-CCR7 therapy in xenograft models is effective in minimizing both frequency and volume of MCL tumors, likely as a result of inhibited migration and subsequent apoptosis[5].

1.3 Tumor Microenvironment

The tumoral microenvironment is the mixture of tumor cells and host cells and the environment that they form[6]. The microenvironment primarily consists of immune cells, stromal cells, vessels and connective tissue and is crucial in deciding growth and survival of tumors and is to be considered when weighing therapeutic target in lymphomas [6]. In B-cell lymphomas, interplay and adhesion with stromal cells enables modification of the gene expression resulting in development of resistance and tumor growth[7]. In MCL the tumor cells interact with both immunal and stromal cells which triggers cellular signaling pathways, which can in turn change the gene expression. The tumor microenvironment affects the epigenome of tumor cells, which can be induced to promote oncogenes. Changes to the epigenome are highly dynamic and is constantly affected by extracellular signals. The modifications are carried out by different enzymes which have in turn been identified as possible therapeutic targets, aiming to reverse upregulation of oncogenes in order to halt aberrant proliferation.

1.4 Chromatin Structure

Chromatin is the basic structure that scaffolds the chromosomal DNA of eukaryotes[8]. The chromatin complex is constructed of repeating nucleosomes around which the DNA helix wraps[9]. The nucleosome consists of the four core histones H2A, H2B, H3 and H4 arranged in octamers[9]. Chromatin can be categorized into heterochromatin and euchromatin, where heterochromatin is a tightly packed structure which limits transcription of the contained genes and euchromatin is a relaxed structure where the DNA helix loosely packed[9]. Thereby the transcriptional machinery is either denied or given access to the

DNA strand, enabling and disabling transcription of the associated genes[10].

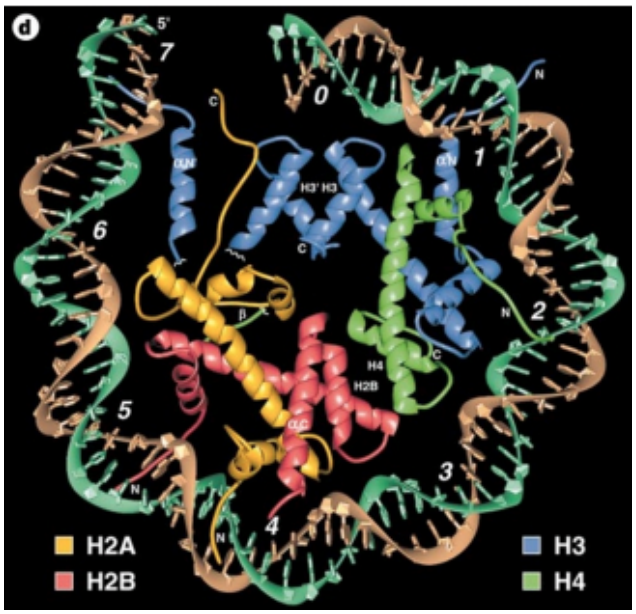

Figure 1: Graphic of the crystal structure of chromatin, from [9]. The N-terminal tails are shown extruding through the DNA helix (N).

Each core histone can be divided up into a histone fold domain and an N-terminal tail[9]. The fold domains allow dimerization between H2A and H2B as well as H3 and H4, maintaining the structural integrity of the nucleosome[8]. It has been demonstrated that N-terminal tails portrude from the nucleosome and interact with nearby nucleosomes, thus affecting the higher level structure of the chromatin[9]. The N-terminal tails can be subject to modulation which changes the tail interaction between nucleosomes, which in turn changes the higher level structure of chromatin[10]. Thus, depending on the state of the N-terminal tail the chromatin packs either as euchromatin or heterochromatin which in turn regulates expression of the genes in the region [8].

1.5 N-terminal tail modification

The packaging properties of the histones are subject to post-translational modulation in a dynamic regulation of the groups and complexes that bind to the amino acids of the N-terminal tails[10]. Modifications are carried out by various enzymes and common changes include methylation, phosphorylation and acetylation[10]. Methylation can occur

by addition of one, two or three methyl groups and depending on the amino acids that are methylated, different enzymes lay down the mark[10]. Methylation primarily occurs on either lysine or arginine and depending on which specific lysine or arginine that is marked, higher level chromatin packaging is affected differently[10]. Should tri-methylation on lysine 4 of Histone 3 (H3K4me3) occur, the chromatin will relax into euchromatin and gene transcription in the region will increase[10]. In contrast, if tri methylation occurs on lysine 27 on histone 3 (H3K27me3) the chromatin packs tighter into heterochromatin which is in turn associated with decreased transcription[10].

H3K27me3 is a mark laid down by the enhancer of zeste homolog 2 (EZH2) enzyme[10]. Thus, expression of EZH2 can be associated with a decrease in gene expression[10]. Likewise, H3K27me3 is removed by the histone-lysine demethylase KDM6B.Depending on the tumor microenvironment, KDM6B has identified both as an oncogene and a tumor suppressing gene[11]. In malignant B-cells from patients diagnosed with MCL, Nuclear Factor Kappa light-chain-enhancer of activated B cells (NFκB) has been identified as a signaling pathway promoting transcription of migration and adhesion related genes, specifically CCR7. In MCL, (NFκB) is assessed to be transcribed when H3K4me3 is not laid down[11]. This has been associated with an over-expression of KDM6B[11]. Disabling CCR7 through antibody treatment has showed repressed dissipation of MCL cells and reduced probability of death in mice[11].

1.6 GSK-J4

GSK-J4 is a histone lysine demethylase inhibitor targeting H3K27me3 demethylase KDM6B[12]. As demonstrated by Heinemann *et al.* GSK-J4 is not inherently specific to KDM6B/A but also demonstrates a weaker inhibition of other demethylases [13]. Generally, dysregulation of H3K27me3 has been identified as a biomarker for hematopoetic malignacies, including MCL[14]. While not exhibiting hyperspecificity towards KDM6B, GSK-J4 has been demonstrated reversing the upregulation of KDM6B in acute myeloid leukemia as well as multiple myeloma *in vitro* resulting in increased H3K27me3 marking and subse-

quent apoptosis[15]. The same study also demonstrated GSK-J4 obstructing tumor cell growth of AML *in vivo* in mouse xenografts[15]. Considering the potential of GSK-J4 as an inhibitor of H3K27me3 demethylase KDM6B it would be of interest to investigate the impact of GSK-J4 on expression of cell surface receptor CCR7 in an MCL cell line.

1.7 Aim

The aim of the study is to investigate the effects of GSK-J4 on cell surface receptor CCR7 expression in MCL cells through analysis of CCR7 levels in cells of the JeKo-1 cell line, in order to determine the therapeutic potential of GSK-J4 in treatment of MCL. The secondary aim is to evaluate the transcription of CCR7 and assess divergence between transcription and expression of CCR7 by analyzing RNA concentration in JeKo-1 treated with GSK-J4.

2 Method

To assess expression of CCR7 and comparatively analyze the effect of GSK-J4 in MCL, cells of the JeKo-1 strain were analyzed using fluorescence-activated cell sorting (FACS). FACS is preferred over a more traditional western blot as it allows multiplexing, several analysis on a single particle at the same time. In order to assess transcription of CCR7, quantitative PCR (qPCR) was used. Both a negative and positive control was used. For the positive control lipopolysaccharides (LPS) were used. Negative control omitted the treatment.

10 µL of cells from the JeKo-1 strain were mixed with 10 µL of trypan blue and counted using an automatic cell counter (ThermoFisher Countess 3). The cells were diluted to contain approximately $10^6 \mathrm{mL}^{-1}$ cells.

2.1 Treatment with GSK-J4

Three samples of 10 µL of JeKo-1 cells at a concentration of $10^6 mL^{-1}$ cells were treated with GSK-J4 and LPS respectively, while one sample was left untreated as a negative control. GSK-J4 (Sigma-Aldrich) and LPS (Sigma-Aldrich) was pipetted into RNAse free eppendorf tubes. GSK-J4 was diluted with dimethyl sulfoxide (DMSO) to a final concentration 10 nM, and LPS was diluted with DMSO to a final concentration of 100 nM. The eppendorf tubes were vortexed for 5 seconds and incubated at 37 °C for 24 hours.

2.2 qPCR assay

2.2.1 RNA extraction

In order to assess the transcription of CCR7 in MCL cells, an assay of RNA levels for the GSK-J4, LPS and control samples was administered. Incubated samples were centrifuged for 6 minutes at $2,500$ rpm and the supernatant was aspirated. 600 µL of TRIzol (Sigma Aldrich) was added and the lysate was vortexed for 5 seconds. The tubes were left at room temperature for 10 minutes. 200 µL of chloroform was added and by turning them upside down 8 times the tubes were mixed carefully. The lysate was left at room temperature for 10 minutes and then centrifuged at 4 °C at 10,000 rpm for 20 minutes. This formed three-phased tubes with a clear aqueous top layer, a middle layer of white precipitated DNA and a bottom pink organic layer. The top layer was pipetted and placed in a separate eppendorf tube, careful so as not to withdraw any precipitated DNA which would contaminate the samples. The withdrawn aqueos phase was diluted 2X with isopropanol and gently mixed. The mixtures were left at room temperature for 10 minutes and subsequently centrifuged at 10,000 rpm for 30 minutes at 4 °C. Pellet formation was observed and samples were placed on ice. Isopropanol was removed and the pellet was washed with 100 µL of 99 % ethanol and recentrifuged at 4 °C for 1 minute. The ethanol was withdrawn and the process was repeated twice. After the last repetition the remaining ethanol was

evaporated and the RNA pellet was dried. After drying but before crystallization occurs, 20 µL of DNase/RNase free water was added to the eppendorf tubes who were in turn vortexed and centrifuged for 5 seconds respectively and placed on ice.

2.2.2 RNA concentration

Using a nanodrop (Implen NanoPhotometer®) the RNA concentration was assessed. The sensor was cleaned with water and tissue and a blank using 2 µL of RNA free water was run. 2 µL of each sample was run on the nanodrop, and the total RNA concentration was analyzed.

2.2.3 Complimentary DNA synthesis

GSK-J4, LPS and control RNA samples were used to synthesize complimentary DNA (cDNA) in order to run qPCR. RNA is not able to amplify in qPCR and thus cDNA is synthesized. This is done using a reverse transcriptase enzyme as well as random sequences of base pairs (random hexameres). The reverse transcriptase synthesises single stranded DNA complimentary to the existing RNA strand, forming a copy of the extracted RNA.

A 2X Reverse Transcription Master Mix was prepared using Applied Biosystems Kit for High Capacity cDNA. Per well, 2 µL of 10X RT Buffer, 2 µL 10X Random Hexamere Primers, 1 µL Reverse Transcriptase and 0.5 µL of dNTP was added to the master mix, calculated for 5.5 µL of master mix per sample. RNA was deposited to each sample to contain 1 µg of RNA per well, calculated using the RNA concentrations obtained in the RNA concentration analysis. Some salt impurities were noted but not sufficient to affect cDNA synthesis. See appendix A for concentration plots.

5.5 µL of master mix and RNA was added to each well. Wells were filled with water to contain a total 20 µL of reaction mixture. The plate was centrifuged briefly and run in a thermal cycler programmed as demonstrated in 1 in order to facilitate synthesis of cDNA. Synthesis occurs in step 2 and the subsequent heat shock in step 3 halts transcription and seals the ends of cDNA. 1 µL of RNA in each well of 20 µL yields a concentration

of 50 ngµL^{-1}. An expected conversion of RNA to cDNA after synthesis is 5 – 10% and cDNA concentration was thus calculated at 5 ngµL^{-1}.

Settings:	**Step 1**	**Step 2**	**Step 3**	**Step 4**
Temperature [°C]	25	37	85	4
Time [min]	10	120	5	Hold

Table 1: Program for cDNA synthesis in ThermoCycler

2.2.4 qPCR

qPCR works by amplifying specific genes using forward and reverse primers custom made to match the gene of interest. When new strands are synthesized a special pigment binds to the new DNA strand and fluoresces. Each fluorescence is detected and thus the growth can be detected in real time. The gene of interest is amplified as well as a house keeping gene. The house keeping gene used as a comparison is expected to be unaffected by the treatment, in this case GSK-J4 and LPS. Both master mixes were prepared for a total of 30 wells using the quanities displayed in Table 2. The primers for CCR7 were special made using UC Santa Cruz's database (Forward: TGAGGTCACGGACGATTACAT, Reverse: GTAGGCCCACGAAACAAATGAT).

Component	**Volume [µL]**
RNase free water	145
SYBR green	180
F-Actin/CCR7 Primer	40

Table 2: Table of ingredients for the master mix used in qPCR of JeKo-1 cells

cDNA of GSK-J4, LPS and control samples was diluted 2X to a concentration of 2.5 ngµL^{-1} and 2 µL of compound was distributed in triplicates in each well of a 96 well plate so as to have 5 ng of cDNA per welL. 10 µL of CCR7 or F-Actin Master Mix was added to the respective cells so as each variant of cDNA had triplicates with each primer at a total of well volume of 12 µL. The plate was centrifuged for 20 seconds to ensure even distribution in the wells and was run in a StepOnePlus RT PCR initiated by denaturation at 95°C followed by an annealing and extension phase at 60 °C repeated for 40 cycles.

Results were analyzed using StepOnePlus 2.1 software which allowed detection of cycle threshold values (CT), the number of cycles required to break a fluorescence threshold value in place to eliminate background noise, for the different genes. If more cDNA is present for a specific gene the CT value will be lower as it requires less cycles to amplify and fluoresce past the threshold. The difference between CT values of CCR7 (ΔCT) and the house keeping gene F-Actin was analyzed using

$$\Delta CT = CT_{F-actin} - CT_{CCR7} \tag{1}$$

and the ΔCT value was base 2 log transformed ($2^{-\Delta CT}$) to normalize the data set, as it is not expected to be normally distributed. Normalized ΔCT values for GSK-J4, LPS and control samples could then be compared to the ΔCT value of F-actin.

2.3 FACS assay

FACS enables sorting of cells based on the scatter of light as well as the fluorescence of special antibodies that bind to cell surface receptors. Cells are passed in a stream in front of lasers of differing wavelengths and the pigment in the antibodies is excited. Scatter is detected by sensors which can be used to analyze both size and cell contents.

2.3.1 Antibody Titration

When using FACS as a method of analysis, gene specific fluorescent antibodies are used for event detection. Antibodies bind to the gene that is analyzed and when excitation by laser occurs they fluoresce, which is in turn detected by the sensors of the FACS machine. Calibration of the amount of antibodies is essential in obtaining accurate results as an oversaturation of antibodies will create background that reduces the resolution of the results, while under-dosing will result in under detection of the cells passing the laser. This analysis used a PE conjugated CCR7 antibody that had not previously been used in analysis of JeKo-1 and thus a calibration was necessary. Dilutions of 1%, 2%, 3%, 5% and

10% were analyzed with a fixed concentration of JeKo-1 cells in order to determine the optimal concentration for separation. This was done through graphing the percentage of PE positive events and identifying where the increase in percentage of PE-positive events, the slope, decreases. As show in Figure 2 a solution of 5% , or 1:20, is optimal for separation as increases beyond that no longer results in a substantial increase in PE-positive events. Thus, this was used for the FACS multiplex assessment of CCR7 levels in JeKo-1. Events were gated to eliminate debris and background, and gating for single cell events was performed to eliminate doubletes (clumped cells). See appendix B for gating strategies for the respective samples.

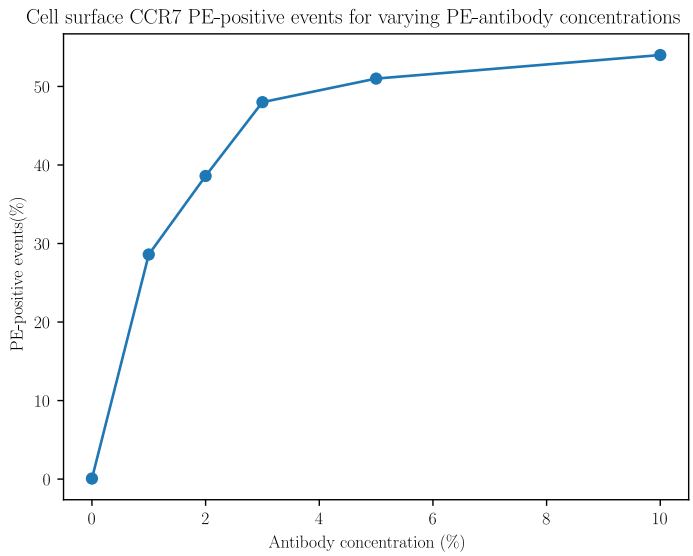

Figure 2: Showing percentage of PE-positive events for the antibody titration of PE-CCR7 for varying concentrations

2.3.2 FACS

Cells from the JeKo-1 cell line were counted at a concentration of $2.36 \times 10^6 \mathrm{mL}^{-1}$ and diluted 10X. GSK-J4 from a stock solution was diluted to 10 nM and stock LPS was diluted to 100 nM. 50 µL of cell solution was deposited into 12 wells respectively in a 96-well plate and a gradient of volumes of GSK-J4 and LPS was added. GSK-J4 volumes were 0.2 nM, 0.4 nM, 0.5 nM, 0.8 nM and 1 nM and LPS was 1 nM, 2 nM and 3 nM.

Cells were left to incubate over night. PE-CCR7 antibodies were added to each well to a final concentration of 1:20 and the plate was shaken for 15 minutes under aluminum foil so as not to degrade the fluorescence of the antibodies. The plate was refrigerated under aluminum foil and run through a MACSQuant Analyzer 10 FACS with high flow. Events were gated to eliminate debris and background. Gating for single cell events was performed to eliminate doubletes (e.g. clumped cells) and to separate PE-positive and negative events, with positive events indicating that fluorescent antibodies were detected. The percentage of PE-positive events of CCR7 can then be compared for the different concentrations. See appendix C for gating strategies for the respective samples.

3 Results

Results for FACS are shown as a comparison between the amount of PE-positive events for the house keeping gene Actin and CCR7. qPCR results show mean cT values for CCR7 for compunds treated with GSK-J4, LPS and control samples.

3.1 FACS assay

Figure 3 shows percentage of PE-positive events for varying concentrations of GSK-J4, including a negative control, demonstrating a decrease in PE positive events as the concentration of GSK-J4 increases. The negative control shows that no PE-positive events were detected when no JeKo-1 cells were present.

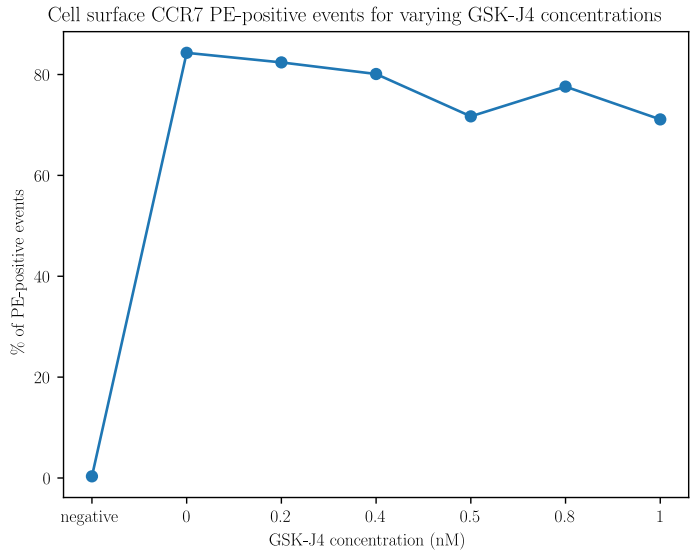

Figure 3: Percentage of PE-postive events for varying concentrations of GSK-J4, including a negative control, from FACS.

Figure 4 shows PE-positive events for varying concentrations of LPS and the negative control. This demonstrates an increase in PE-positive events as the concentration of LPS is increased. The negative control shows that no PE-positive events were detected when no JeKo-1 cells were present.

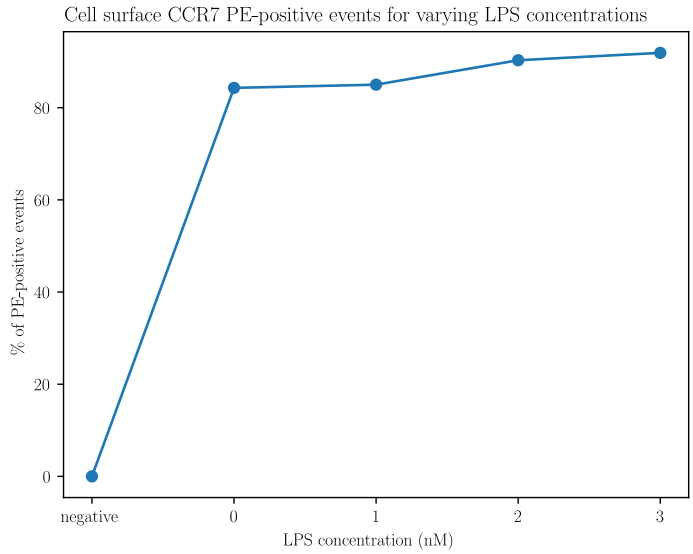

Figure 4: Percentage of PE-postive events for varying concentrations of LPS, including a negative control, from FACS.

3.2 qPCR assay

Figure 5 shows the average log transformed ΔCT values for the respective samples, showing that cDNA for CCR7 in GSK-J4 and LPS took longer to amplify past the noise threshold compared to the control. Since the sample size was too low to obtain standard deviations, standard error of the mean was generated for error bars showing the largest error for the control sample.

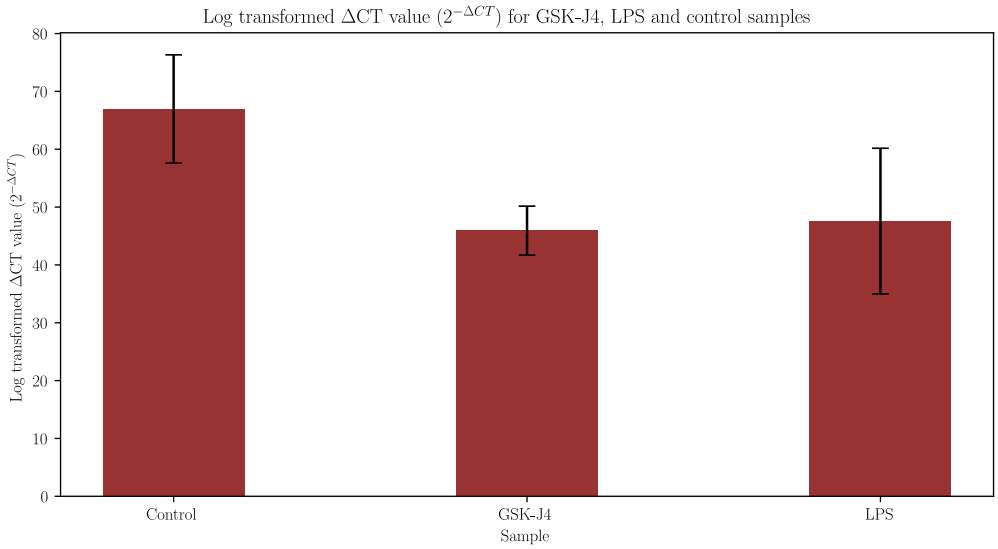

Figure 5: Average log transformed ΔCT values for the control, GSK-J4 and LPS samples obtained using qPCR of cDNA samples, with error bars generated using the standard error of the mean.

4 Discussion

An overall decrease in both transcription and translation of CCR7 in JeKo-1 can be observed when cells are treated with GSK-J4. LPS transcription is decreased while translation increases. Most importantely, statistical signficance could not be demonstrated due to low sample sizes as a result of a time constraints, and thus meaningful conclusions regarding the efficacy of GSK-J4 could not be drawn.

4.1 RNA assay

The results in Figure 5 indicate a decrease in transcription of CCR7 as a result of treatment with GSK-J4 when compared with the control. Likewise, a decrease in the transcription of LPS can be noted as seen in figure 5. This contradicts the expectation of LPS acting as an enhancer of CCR7. However, it should be considered that the standard error of the mean values demonstrated a large variance in the results. This variance is especially prevalent in the control group which complicates any comparisons with GSK-J4 and LPS treated samples. Due to time constraints, only technical replicates were carried out and therefore acquiring statistical significance is out of scope for this study. Biological replicates are preferred as they use different sub populations of cells and therefore show a variance in the population, more comparable to the real world. This reduces the risk of results being limited to specific subset population of cells. Further research would have to carried out on transcription levels of CCR7 after treatment with GSK-J4 and LPS to draw any meaningful conclusions, but a decrease in transcription is not necessarily linked to a decrease in translation which should be examined independenty.

4.2 FACS assay

Figure 3 demonstrates a decrease in expression of CCR7 on the cell surface of JeKo-1 as the concentration of GSK-J4 increases, indicating a result that confirms the effectiveness of GSK-J4 as an indirect inhibitor of CCR7 in MCL. This is in line with previous research suggesting GSK-J4 as an inhibitor for KDM6B, resulting in an increase of H3K27me3 markings. This would in turn lead to a transformation to heterochromatin, decreasing expression of the NFκB pathway which in turn down-regulates CCR7 as seen in figure 3, which would be the likely explanation for the results obtained. However, due to time constraints, no biological replicates were examined and no statistical tests could be done. Despite this, an indication can indeed be observed which should incentivize further research including biological replicates and different cell lines. Figure 4 shows the increase

in CCR7 expression as the LPS concentration increases. This falls in line with the expectation of LPS as an enhancer of CCR7. This stands in contrast to the decrease shown in figure 5, demonstrating a decrease in transcription but an increase in translation. While counter intuitive, this could be attributed to LPS promoting reuse of activated CCR7 and preventing degradation, thus increasing expression. The decrease in transcription could be explained by feed forward inhibiton mechanisms that come into effect when CCR7 is already present on the cell surface.

4.3 Implications

The demonstrated decrease in both translation and transcription of CCR7 in MCL cells as a result of GSK-J4 treatment may suggest a possible use for GSK-J4 as a treatment for MCL. Increased inhibition of CCR7 would reduce probability of migration to the lymph nodes of malignant B-cells, decreasing the amount of cells protected from chemotherapy but also minimizing the cells that reach their niche. This could in turn lead to reduced proliferation of malignant B-cells, inducing apoptosis. Preventing MCL cells from reaching their niche could increase efficacy of chemotherapy treatment leading to longer remissions and decreased risk of relapse. Thus, GSK-J4 could demonstrate therapeutic potential for synergistic use with other drugs, as has been suggested for other lymphomas as well as acute myeloid leukemia.

4.4 Further research

Since the study cannot demonstrate statistical significance for neither the decreased transcription nor translation of CCR7 due to low sample sizes, the first aim should be to verify the results with biological replicates and demonstrate statistical significance. Should the results be verified, examination on different cell lines such as CCMCL1 or Mino can be carried out. Once verified to a satisfactory degree, research could proceed to *in vivo* experiments. A proposed method that has been used in examination of AML is a human

xenograft model in mice. Examining potential side effects of GSK-J4 both on MCL cells and host cells in the tumoral microenvironment is necessary in *in vivo* testing. The primary purpose of further research should be to decide viability of GSK-J4 as a therapy for MCL.

4.5 Conclusion

In conclusion, the study demonstrates a decrease in both transcription and translation of CCR7 in the MCL cell line JeKo-1 after treatment with the compound GSK-J4. However, since the scope of the study was limited to a proof of theory no statistical significance can be granted to the results and no meaningful conclusions can be drawn. The results could indicate GSK-J4 as a potential complimentary treatment for MCL, though further research needs to be conducted in order to achieve statistical significance before any such conclusions can be drawn.

References

[1] Ward JM, Cherian S, Linden MA. 19 - Hematopoietic and Lymphoid Tissues. In: Treuting PM, Dintzis SM, Montine KS, editors. Comparative Anatomy and Histology (Second Edition). second edition ed. San Diego: Academic Press; 2018. p. 365-401. Available from: https://www.sciencedirect.com/science/article/pii/B9780128029008000191.

[2] Nichols CR. In: Fisch MJ, Bruera E, editors. Hodgkin's and non-Hodgkin's lymphoma. Cambridge University Press; 2003. p. 308–316.

[3] Pérez-Galán P, Dreyling M, Wiestner A. Mantle cell lymphoma: biology, pathogenesis, and the molecular basis of treatment in the genomic era. Blood. 2011;117(1):26-38. Available from: https://www.sciencedirect.com/science/article/pii/S0006497120601379.

[4] Pu J, Savani M, Huang N, Epner E. Mantle cell lymphoma management trends and novel agents: where are we going? Therapeutic Advances in Hematology. 2022 02;13:204062072210807.

[5] Somovilla-Crespo B, Alfonso-Pérez M, Cuesta-Mateos C, Carballo de Dios C, Beltrán A, Terrón F, et al. Anti-CCR7 therapy exerts a potent anti-tumor activity in a xenograft model of human mantle cell lymphoma. Journal of hematology and oncology. 2013 12;6:89.

[6] Anderson N, Simon M. The tumor microenvironment. Current Biology. 2020 08;30:R921-5.

[7] Scott DW, Gascoyne RD. The tumour microenvironment in B cell lymphomas. Nature Reviews Cancer. 2014 Aug;14(8):517-34. Available from: https://doi.org/10.1038/nrc3774.

[8] Mariño-Ramírez L, Kann M, Shoemaker B, Landsman D. Histone structure and nucleosome stability. Expert review of proteomics. 2005 11;2:719-29.

[9] Luger K, Mäder A, Richmond R, Sargent D, Richmond T. Luger, K., Mader, A.W., Richmond, R.K., Sargent, D.F. and Richmond, T.J. Crystal structure of the nucleosome core particle at 2.8 Å resolution. Nature 389, 251-260. Nature. 1997 10;389:251-60.

[10] Bannister A, Kouzarides T. Bannister AJ, Kouzarides T. Regulation of chromatin by histone modifications. Cell Res 21: 381-395. Cell research. 2011 02;21:381-95.

[11] Sadeghi L, Wright AP. Migration and Adhesion of B-Lymphocytes to Specific Microenvironments in Mantle Cell Lymphoma: Interplay between Signaling Pathways and the Epigenetic Landscape. International Journal of Molecular Sciences. 2021;22(12). Available from: https://www.mdpi.com/1422-0067/22/12/6247.

[12] Kruidenier L, Chung Cw, Cheng Z, Liddle J, Che K, Joberty G, et al. A selective jumonji H3K27 demethylase inhibitor modulates the proinflammatory macrophage response. Nature. 2012 Aug;488(7411):404-8. Available from: https://doi.org/10.1038/nature11262.

[13] Heinemann B, Nielsen JM, Hudlebusch HR, Lees MJ, Larsen DV, Boesen T, et al. Inhibition of demethylases by GSK-J1/J4. Nature. 2014 Oct;514(7520):E1-2.

[14] Ueda T, Nakata Y, Nagamachi A, Yamasaki N, Kanai A, Sera Y, et al. Propagation of trimethylated H3K27 regulated by polycomb protein EED is required for embryogenesis, hematopoietic maintenance, and tumor suppression. Proceedings of the National Academy of Sciences. 2016;113(37):10370-5. Available from: https://www.pnas.org/doi/abs/10.1073/pnas.1600070113.

[15] Li Y, Zhang M, Sheng M, Zhang P, Zizhen C, Xing W, et al. Therapeutic potential of GSK-J4, a histone demethylase KDM6B/JMJD3 inhibitor, for acute myeloid leukemia. Journal of Cancer Research and Clinical Oncology. 2018 06;144.

Appendix

Appendix A

Implen NanoPhotometer®

Instrument	NP80
Version	NPOS 2.0a build 12465
Serial Number	M80804
Self-test passed	2022-06-21; 09:16

Parameter

Method	Nucleic Acids	Nucleic Acid Factor	40.00
Type	RNA	Background Correction	On
Mode	NanoVolume	Air Bubble Recognition	Off
Volume (ul)	1-2	Manual Dilution factor	1.000

#	Name	Conc.	Units	A230	A260	A280	A320	A260/A280	A260/A230	Dilution
1	Blank 1	0.0000	ng/ul	0.000	0.000	0.000	0.000	0.000	0.000	
2	Ctrl	108.64	ng/ul	2.324	2.729	1.500	0.013	1.826	1.175	15
3	Gskj4	129.56	ng/ul	3.809	3.253	1.775	0.014	1.839	0.853	15
4	LPS	115.04	ng/ul	2.311	2.882	1.680	0.006	1.718	1.248	15

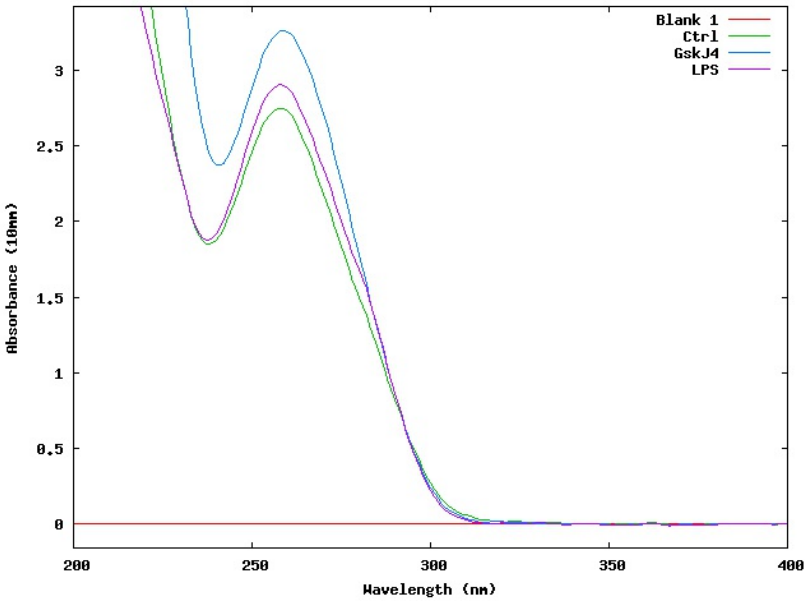

Result 1 / 1 2022-06-29 13:54:11

Implen NanoPhotometer®

Instrument	NP80
Version	NPOS 2.0a build 12465
Serial Number	M80804
Self-test passed	2022-06-21; 09:16

Parameter

Method	Nucleic Acids	Nucleic Acid Factor	40.00
Type	RNA	Background Correction	On
Mode	NanoVolume	Air Bubble Recognition	Off
Volume (ul)	1-2	Manual Dilution factor	1.000

#	Name	Conc.	Units	A230	A260	A280	A320	A260/A280	A260/A230	Dilution
1	Blank 1	0.0000	ng/ul	0.000	0.000	0.000	0.000	0.000	0.000	
2	ctrl	318.12	ng/ul	16.47	8.005	4.640	0.052	1.733	0.484	15
3	Gsk	391.24	ng/ul	11.66	9.814	5.571	0.033	1.766	0.841	15
4	Lps	350.88	ng/ul	15.34	8.795	5.322	0.023	1.655	0.573	15

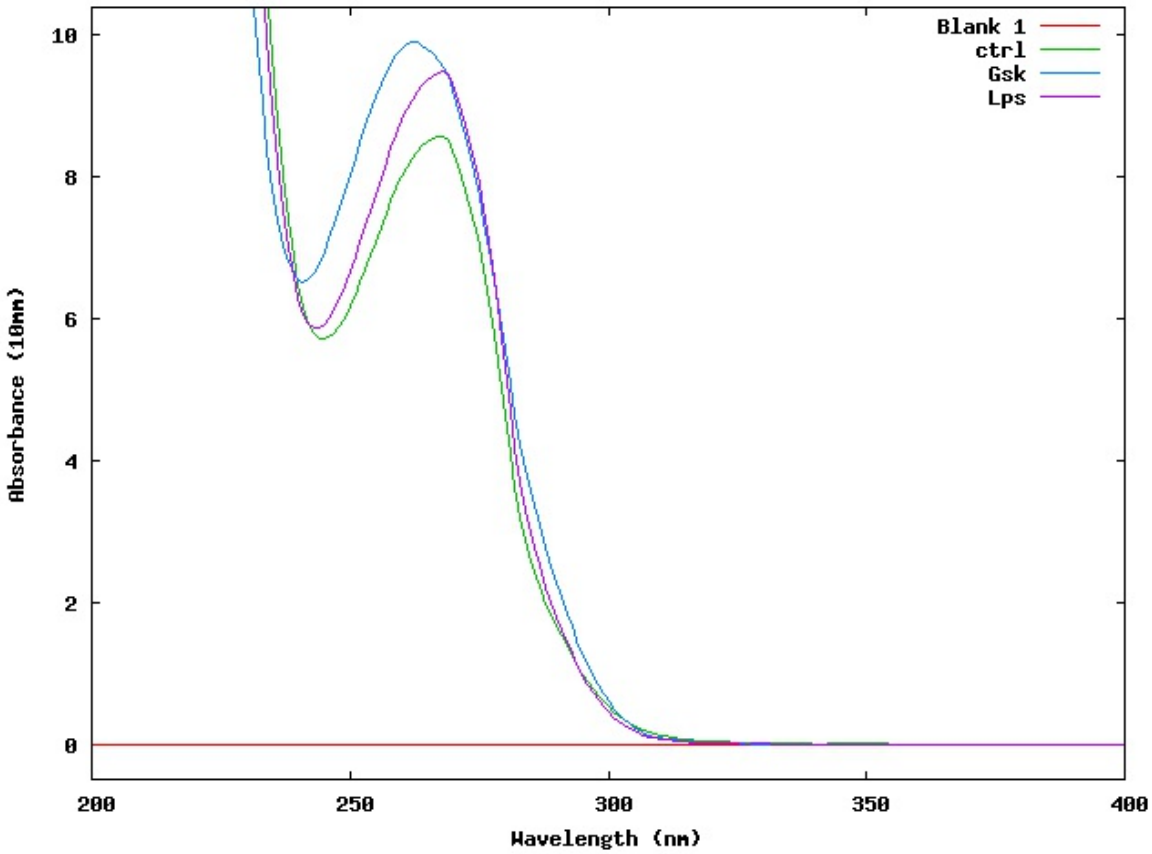

Appendix B

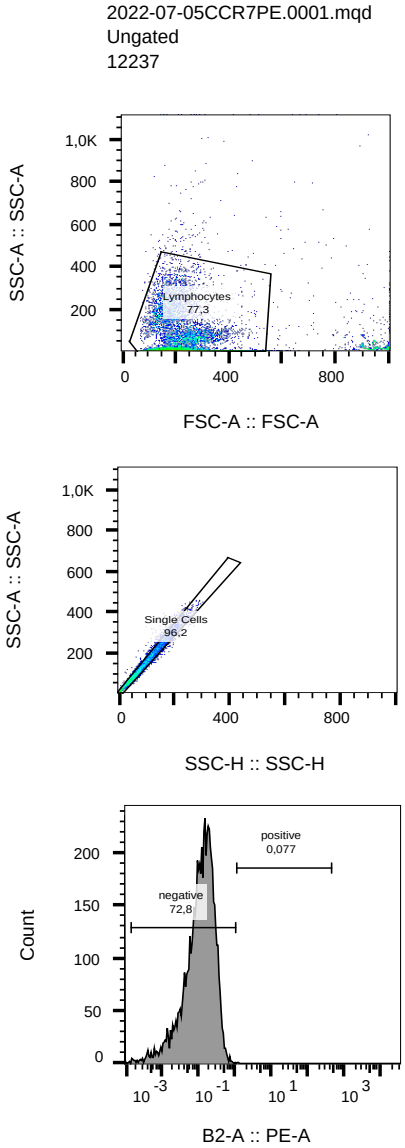
2022-07-05CCR7PE.0001.mqd
Ungated
12237
SSC-A :: SSC-A
1,0K
800
600
400
200
Lymphocytes
77,3
0
400
800
FSC-A :: FSC-A
SSC-A :: SSC-A
1,0K
800
600
400
200
Single Cells
96,2
0
400
800
SSC-H :: SSC-H
Count
200
150
100
50
0
positive
0,077
negative
72,8
10 -3
10 -1
10 1
10 3
B2-A :: PE-A

2022-07-05CCR7PE.0002.mqd
Ungated
15257

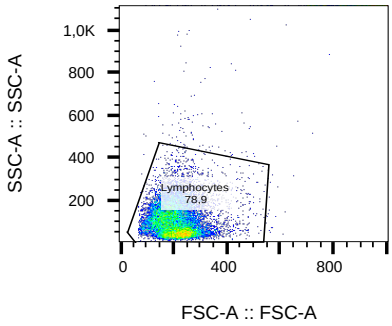

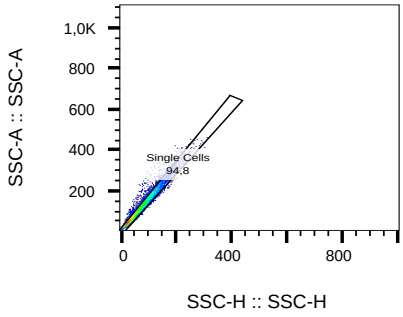

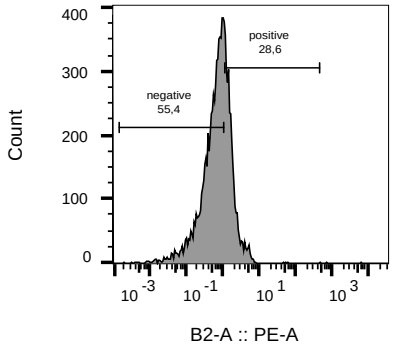

2022-07-05CCR7PE.0003.mqd
Ungated
18232

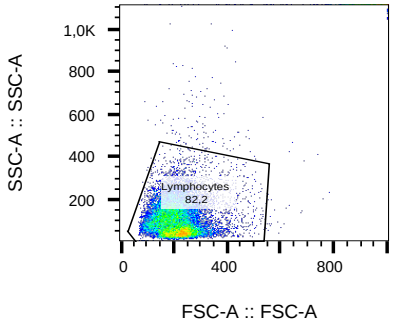

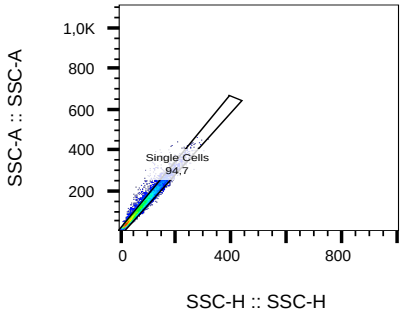

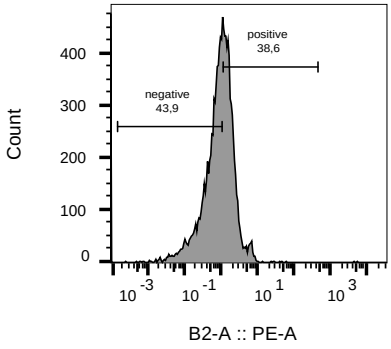

2022-07-05CCR7PE.0004.mqd
Ungated
21071

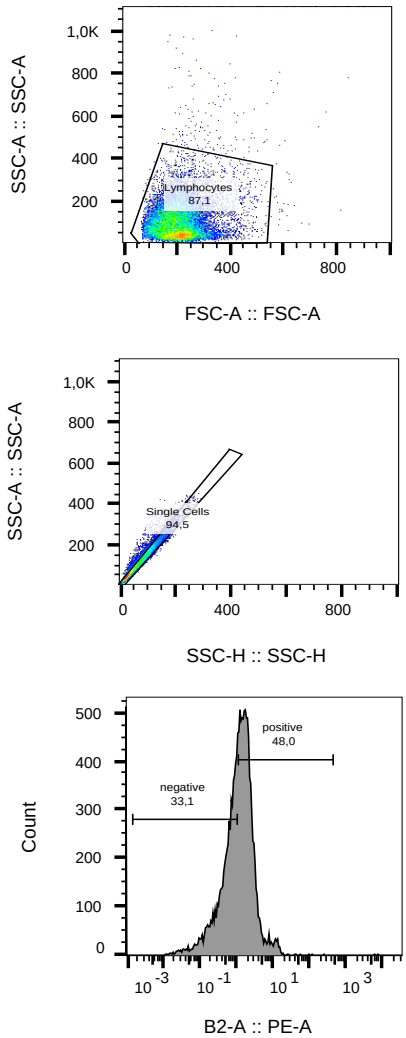

2022-07-05CCR7PE.0005.mqd
Ungated
17992

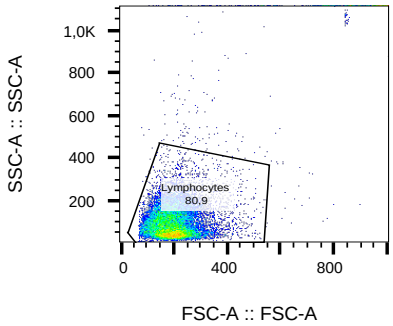

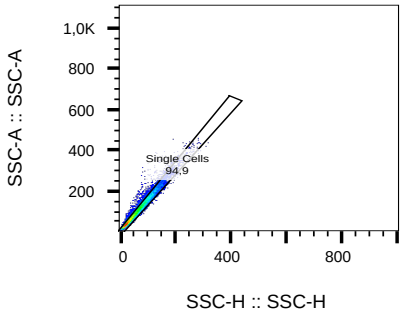

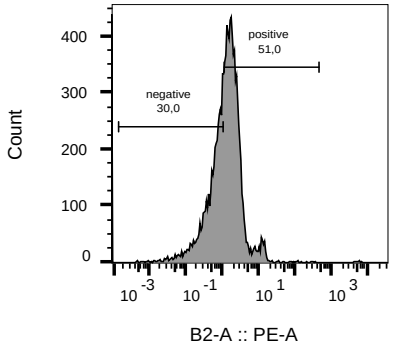

2022-07-05CCR7PE.0006.mqd
Ungated
18742

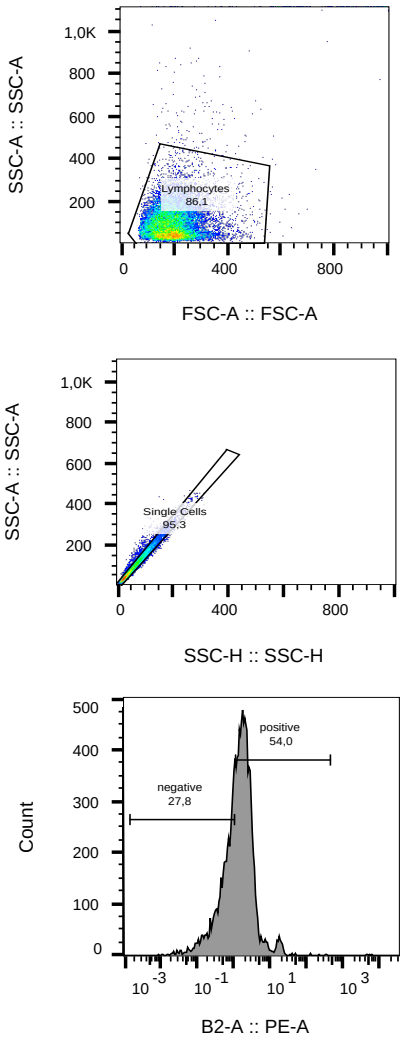

Appendix C

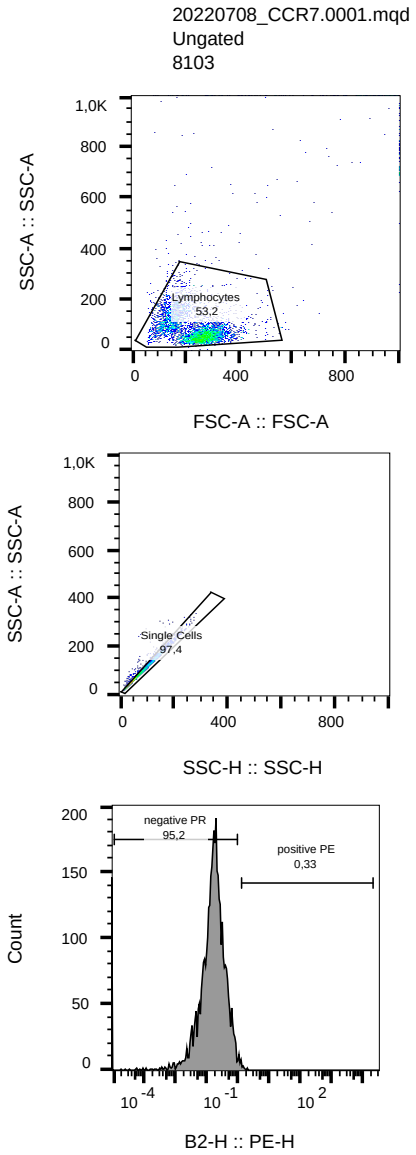
20220708_CCR7.0001.mqd
Ungated
8103
SSC-A :: SSC-A
1,0K
800
600
400
200
0
Lymphocytes
53,2
0
400
800
FSC-A :: FSC-A
SSC-A :: SSC-A
1,0K
800
600
400
200
0
Single Cells
97,4
0
400
800
SSC-H :: SSC-H
Count
200
150
100
50
0
negative PR
95,2
positive PE
0,33
10 -4
10 -1
10 2
B2-H :: PE-H

20220708_CCR7.0002.mqd
Ungated
10000

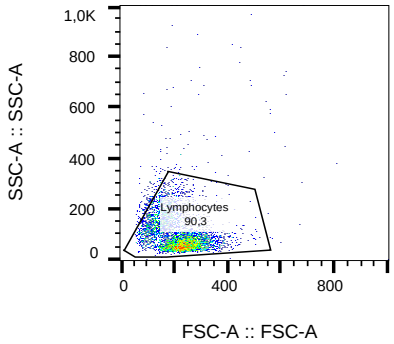

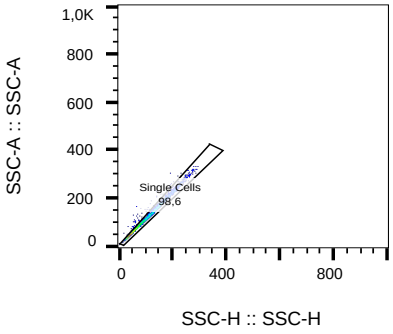

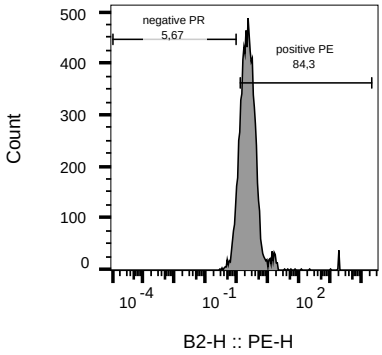

20220708_CCR7.0003.mqd
Ungated
9907

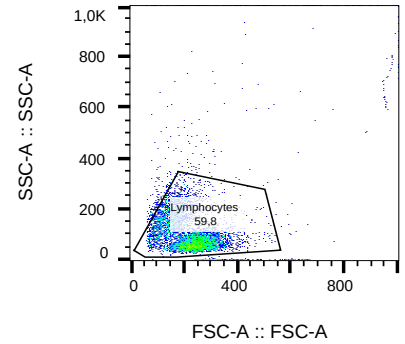

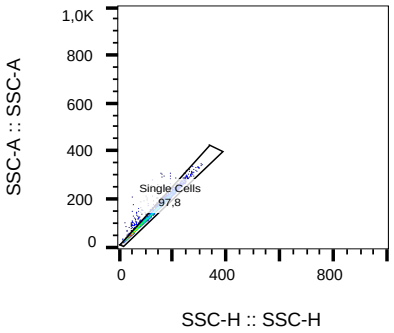

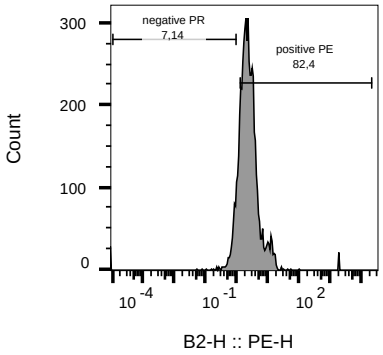

20220708_CCR7.0004.mqd
Ungated
5079

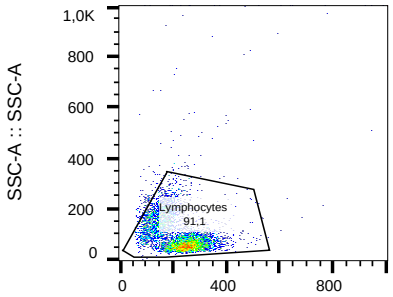

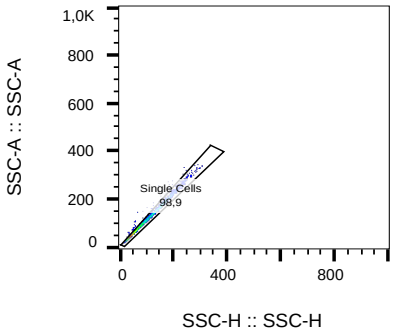

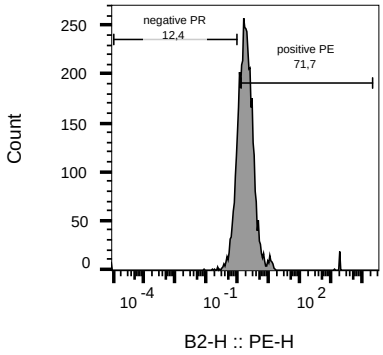

20220708_CCR7.0005.mqd
Ungated
10000

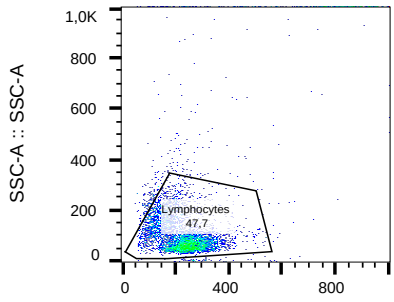

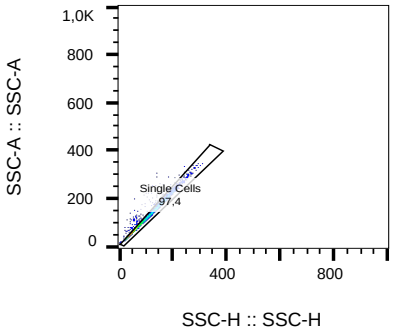

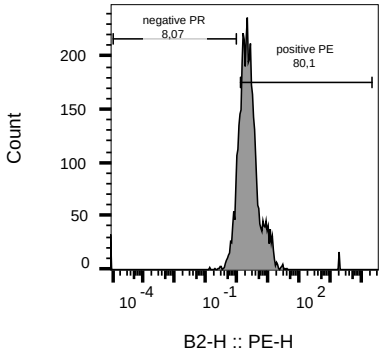

20220708_CCR7.0006.mqd
Ungated
8212

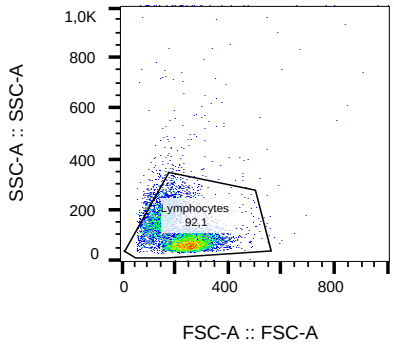

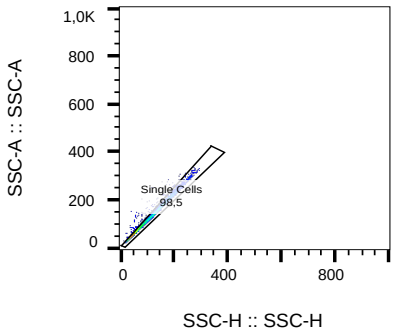

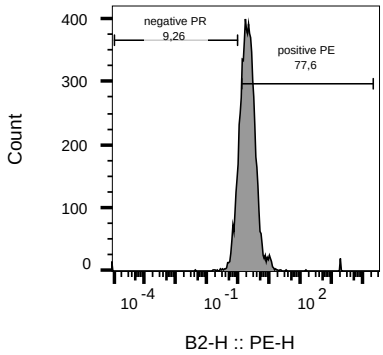

20220708_CCR7.0007.mqd
Ungated
7840

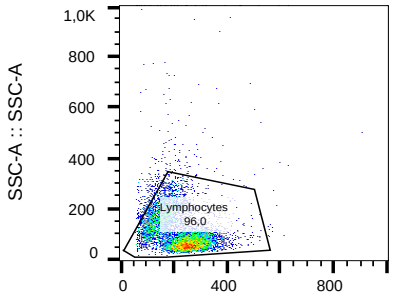

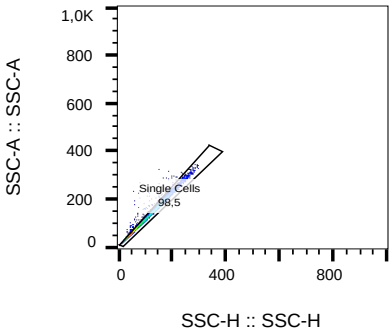

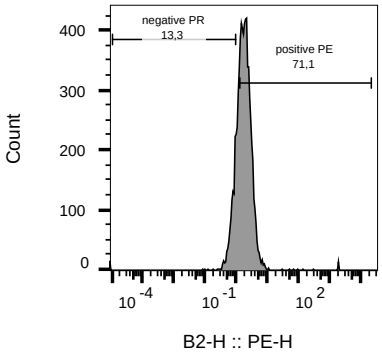

20220708_CCR7.0008.mqd
Ungated
10000

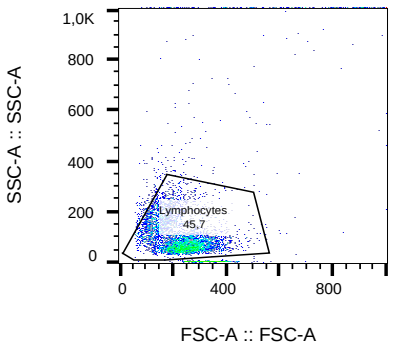

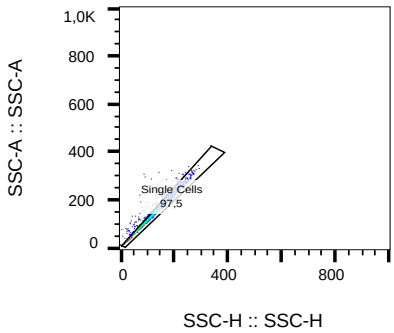

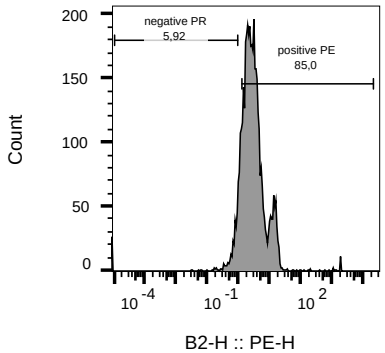

20220708_CCR7.0009.mqd
Ungated
9352

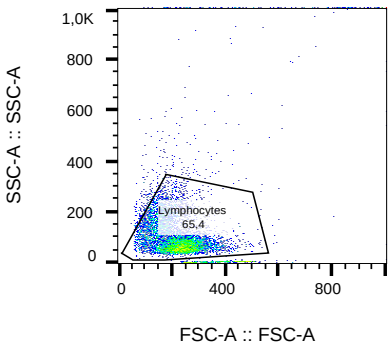

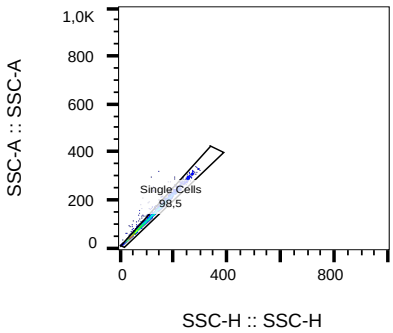

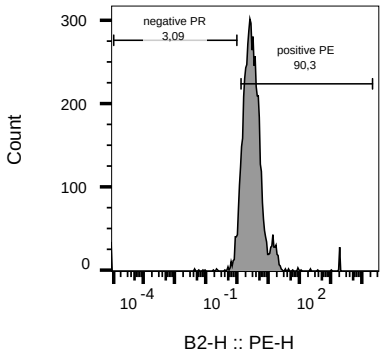

20220708_CCR7.0010.mqd
Ungated
8812